CROP-CENTRIC AGRICULTURAL POTENTIAL OF URBAN SURFACES

A Sunlight-based Computational Approach For Food Security

ALBA LOMBARDIA[1], THOMAS SCHROEPFER[2], ARLINDO SILVA[3] and CARLOS BANON[4]
[1,2,3,4] Singapore University of Technology and Design.
[1,2,4] Architecture and Sustainable Design.
[3] Engineering Product Development.
[1]alba_lombardia@mymail.sutd.edu.sg, ORCID:0000-0002-6489-2541
[2]thomas.schroepfer@sutd.edu.sg,ORCID:0000-0001-5755-7334
[3]arlindo_silva@sutd.edu.sg,ORCID: 0000-0001-5120-3914
[4]carlos_banon@sutd.edu.sg,ORCID: 0000-0002-7408-5639

Abstract. Urban agricultural systems will be configured over the following years to respond to increasing climate change, urbanisation, and population growth. Controlled environment agriculture (CEA) is an increasing trend since it can be easily integrated into the built environment. However, this food production system requires intensive capital and energy resources, with artificial lighting as the primary contributor to its high operational impacts. New methods and tools for planning and design can provide innovative solutions for shifting urban agriculture toward sustainability. This paper addresses the food security challenge in cities by introducing a sunlight-based computational approach for indicating the agricultural possibilities of three-dimensional urban surfaces according to crop-centric environmental suitability. The procedure aims to improve CEA efficiency through a passive natural lighting optimisation strategy, indicating the sunlight thresholds for various crop species. The methodology interconnects solar radiation values measured through sunlight simulations with crops' daily light integrals, using Singapore and Chennai (India) as case studies. The results suggest that urban areas with high solar radiation levels possess large degrees of year-round harvesting potential. This methodology can assist designers (architects, urban planners, and engineers) and local governments in strategizing urban agriculture developments and provide decision-making support for crop harvesting initiatives in cities.

Keywords. Food Security, Urban Agriculture, Solar Radiation, Daily Light Integral, Sunlight Simulation.

1. Introduction

Cities must provide solutions to establish local food security and, at least to some

HUMAN-CENTRIC, Proceedings of the 28th International Conference of the Association for Computer-Aided Architectural Design Research in Asia (CAADRIA) 2023, Volume 2, 573-582.

extent, sustainably feed their citizens. Due to increasing urbanisation, population growth, and climate change, current agricultural systems must be reconfigured, creating proximity between consumption and production while reducing global environmental degradation and deforestation. These concerns have led to a shift from traditional to urban farming. Small-footprint solutions like vertical agriculture were first popularised by Dr Dickson Despommier (Despommier, 2010) in the early 21st century. Since then, the urban farming transformation has been accelerating due to its social, environmental, and economic benefits (Specht et al., 2014). Among its different typologies, Controlled Environment Agriculture (CEA) is an increasing trend in cities worldwide since it can be easily integrated into the built environment. However, critics state that CEA focuses on high-end products that require intensive capital and energy resources. Notably, artificial lighting is the main contributor to the high operational impacts of CEA (Engler & Krarti, 2021). Correspondingly, light is the most basic need for crop production leading to photosynthesis and growth, which is the main objective of agricultural processes. Nevertheless, there is limited academic research on the design of building-integrated agriculture focused on passive natural lighting optimisation. Additionally, crop-specific requirements are commonly disregarded.

New methods and tools for planning and design can provide innovative solutions for sustainable urban agriculture. Recent literature on solar harvesting suggests a large quantity of unexplored solar potential (Zhu et al., 2022) in high-density cities like Singapore. In addition, the city's urban morphology and three-dimensionality significantly affect solar radiation levels due to its highly dense structure with significant oscillations of building heights (Zhu et al., 2020). This paper addresses the food security challenge in cities by introducing a sunlight-based approach for urban agriculture according to crop-centric urban environmental suitability using Singapore and Chennai (India) as case studies. Furthermore, the paper aims to improve CEA systems' efficiency through a passive natural lighting optimisation strategy that indicates the sunlight thresholds for various crop species.

2. Methodology

2.1. SOLAR POTENTIAL OF CITIES

The study considers the underused solar potential of cities from a three-dimensional perspective (façade, roof, and ground levels) toward implementing crop harvesting on urban surfaces. Specifically, contemporary literature on solar accessibility can have different applications, like photovoltaic cells' location for energy harvesting (Zhu et al., 2022). Additionally, there is an intense interdependence between solar potential and urban morphology (Zhu et al., 2020). Previous research indicates the heterogeneous distribution of solar radiation in the built environment, highlighting the value of using spatio-temporal models for analysing the three-dimensional solar capacity of urban surfaces (Zhu et al., 2022).

2.2. PHOTOSYNTHETICALLY ACTIVE RADIATION

Urban studies consider solar radiation (radiant energy from the sun) since the objectives of the investigations usually focus on solar energy harvesting or urban heat island effect mitigation. However, crops cannot absorb the total amount of solar radiation, but a part called Photosynthetically Active Radiation (PAR) correspondent to 42.3% of the total radiation (Fondriest Environmental, 2014). For this reason, this paper considers the differences, similarities, and conversions between both. Current studies usually measure PAR directly with sensors since simulated PAR can have high deviations from sensor-measured PAR results. Indeed, scientific evidence shows how modelled PAR can capture the trend that actual PAR follows but not its values, which are usually underestimated (Palliwal et al., 2021). Nevertheless, empirical formulas obtained from experimental sensorised data (Weiss & Norman, 1985) to calculate PAR from the total incoming solar radiation may be more accurate than simulated results. As a result, this method for estimating PAR was followed in this study.

2.3. CROP SUNLIGHT REQUIREMENTS

Three main factors influence crop growth: light, water, and nutrients. Although artificial light has been broadly studied and optimised concerning crop growth, it is still CEA's primary energy-intensive operational dimension. Therefore, investigating natural lighting passive strategies for future urban agricultural planning has enormous potential. The effect of solar radiation on crop growth has been broadly studied and modelled for traditional extensive outdoor agriculture (Trnka et al., 2007). However, in the built environment, research on adequate exposure to sunlight for crops is in its infancy. It has been studied on facades (Palliwal et al., 2021), rooftops (Nadal et al., 2017), and ground levels (Saha & Eckelman, 2017), but not from a three-dimensional urban surface perspective that considers all surfaces simultaneously along with the lighting growth thresholds of different crop species.

This paper defines the species and their growth lighting thresholds to interconnect the sunlight analysis of urban surfaces with the crop requirements. Crop light requirements are commonly described by Photosynthetic Photon Flux Density (PPFD) or Daily Light Integral (DLI) values. PPFD refers to light intensity. It measures how much density of photons the sunlight is packed with (LEDTonic, n.d.). DLI is the total amount of PAR over 24 hours (Palliwal et al., 2021). Outdoor sunlight DLI can vary from 5 to 60 mol·m-2·d-1 (Torres & Lopez, 2012). According to DLI requirements, crops can be classified into four groups: (1) low-light crops (3-6 mol·m-2·d-1); (2) medium-light crops (6-12 mol·m-2·d-1); (3) high-light crops (12-18 mol·m-2·d-1); and (4) very high-light crops (>18 mol·m-2·d-1) (Torres & Lopez, 2012). This study aims to interconnect the lighting thresholds of the selected 26 crop species (see Table 1) with incident radiation quantities, which is the dimension measured in urban sunlight simulations. First, a simple conversion of the values given in PPF to DLI is made, considering the different photoperiods indicated by the related literature. Second (see Table 1), a succession of conversions is elaborated using empirical formulas to transform DLI values into incident radiation quantities that allow comparing the simulated sunlight values and the daily crop lighting needs.

	CROP			LIGHTING THRESHOLDS			
ID	Type	Specie	Scientific Name	Source	Photoperiod (PPF)	PPF	DLI
					h	$\mu mol \cdot m^{-2} \cdot s^{-1}$	$mol \cdot m^{-2} \cdot d^{-1}$
1	Mushrooms	Oyster	*Pleurotus ostreatus*	**F**	**12**	**12**	0
2	Mushrooms	Shiitake	*Lentinula edodes*	**G**	**12**	**55**	2
3	Berries	Blueberry	*Vaccinium* sect. *Cyanococcus*	**G**	**16**	**100**	6
4	Herbs	Mint	*Mentha spicata*	**A**	12	232	**10**
5	Herbs	Oregano	*Origanum vulgare*	**A**	12	232	**10**
6	Herbs	Rosemary	*Salvia rosmarinus*	**A**	12	232	**10**
7	Microgreens	Cilantro	*Coriandrum sativum*	**D**	12	278	**12**
8	Microgreens	Dill	*Anethum graveolens*	**D**	12	278	**12**
9	Microgreens	Parsley	*Petroselinum crispum*	**D**	12	278	**12**
10	Leafy Greens	Swiss Chard	*Beta vulgaris*	**B**	16	208	**12**
11	Leafy Greens	Kale	*Brassica oleracea var. sabellica*	**B**	16	208	**12**
12	Leafy Greens	Pac Choi	*Brassica rapa var. chinensis*	**C**	16	208	**12**
13	Leafy Greens	Cabbage	*Brassica oleracea var. sabauda*	**B**	12	278	**12**
14	Microgreens	Basil	*Ocimum basilicum*	**E**	12	301	**13**
15	Salad Greens	Lettuce	*Lactuca sativa*	**A**	12	324	**14**
16	Salad Greens	Arugula	*Eruca sativa*	**C**	12	324	**14**
17	Berries	Raspberry	*Rubus idaeus*	**B**	12	347	**15**
18	Leafy Greens	Spinach	*Spinacia oleracea*	**F**	**16**	**295**	18
19	Vine Vegetables	Cucumber	*Cucumis sativus*	**A**	12	463	**20**
20	Vine Vegetables	Pepper	*Capsicum annuum*	**A**	12	463	**20**
21	Berries	Strawberry	*Fragaria × ananassa*	**B**	12	463	**20**
22	Vine Vegetables	Tomato	*Solanum lycopersicum*	**A**	12	509	**22**
23	Legums	Black Bean	*Phaseolus vulgaris*	**F**	**18**	**370**	22
24	Flowering Plants	Sunflower	*Helianthus*	**F**	**16**	**400**	24
25	Flowering Plants	Quinoa	*Chenopodium quinoa*	**F**	**16**	**400**	24
26	Cereals	Asian Rice	*Oryza sativa*	**G**	**12**	**800**	32

	CONVERSIONS						
ID	DLI	Step 1 (Source H) PAR	Step 2 (Source I) Global Radiation (GR)		Step 3 (Source J) Incident Radiation (IR)		
		PAR= DLI / 0.0864	GR= PAR x 2.02		E (IR)= P (GR) x t (h)		
	$mol \cdot m^{-2} \cdot d^{-1}$	$\mu mol \cdot m^{-2} \cdot s^{-1}$	$W \cdot m^{-2}$	$kW \cdot m^{-2}$	$kW \cdot h \cdot m^{-2}$ (day)	$kW \cdot h \cdot m^{-2}$ (year)	$MW \cdot h \cdot m^{-2}$ (year)
1	0	6	11	0.01	0.13	49	0.05
2	2	25	51	0.05	0.62	225	0.23
3	6	69	140	0.14	1.68	614	0.61
4	**10**	116	234	0.23	2.81	1024	1.02
5	**10**	116	234	0.23	2.81	1024	1.02
6	**10**	116	234	0.23	2.81	1024	1.02
7	**12**	139	281	0.28	3.37	1229	1.23
8	**12**	139	281	0.28	3.37	1229	1.23
9	**12**	139	281	0.28	3.37	1229	1.23
10	**12**	139	281	0.28	3.37	1229	1.23
11	**12**	139	281	0.28	3.37	1229	1.23
12	**12**	139	281	0.28	3.37	1229	1.23
13	**12**	139	281	0.28	3.37	1229	1.23
14	**13**	150	304	0.30	3.65	1331	1.33
15	**14**	162	327	0.33	3.93	1434	1.43
16	**14**	162	327	0.33	3.93	1434	1.43
17	**15**	174	351	0.35	4.21	1536	1.54
18	18	205	414	0.41	4.97	1813	1.81
19	**20**	231	468	0.47	5.61	2048	2.05
20	**20**	231	468	0.47	5.61	2048	2.05
21	**20**	231	468	0.47	5.61	2048	2.05
22	**22**	255	514	0.51	6.17	2253	2.25
23	22	257	519	0.52	6.23	2273	2.27
24	24	278	561	0.56	6.73	2458	2.46
25	24	162	327	0.33	3.93	1434	1.43
26	32	370	748	0.75	8.98	3277	3.28

Table 1: Upper part: Selected crop species and corresponding growth lighting thresholds. Sources: (A) Dr L. Morgan (LEDTonic, n.d.); (B) Prof. E. Runkle (LEDTonic, n.d.); (C) (Currey & Yost, 2020); (D)(Currey et al., 2019); (E) (Dou et al., 2018); (F)(Gellenbeck et al., 2019); and (G) (Engler & Krarti, 2021). Bottom part: Converting DLI to Incident Radiation values. Sources: (H) (Torres & Lopez, 2012), (I) (Mavi & Tupper, 2004), and (J) (Irulegi et al., 2014).

2.4. CASE STUDIES

The selected areas of study for the crop-centric methodology described in this paper showcase the strategy's potential for a global incrementation of food security in urban areas. The two geographical areas demonstrate the replicability of the method in different locations, climates, and urban contexts. The climatic conditions of both sites allowed the simplification of the study, running yearly instead of monthly simulations analysis since there are non-pronounced seasons throughout the year. The two case study areas are (1) the Singapore University of Technology and Design campus; and (2) the Hazur Garden area in Chennai, India. Both areas permit the testing of the computational approach at an urban meso scale. The sites have contrasting differences regarding their morphology, landscape and building typology. This dissimilarity in the case studies allows for validating the methodology and establishing generalized conclusions. The validation of the method follows a bottom-up strategy model, in which future city-scale predictions are based on the behaviour of its components, in this case, building blocks located under two varied scenarios.

The digital models used in the case studies have a high level of definition with accurate detail of surrounding buildings and trees. Detailed models considering the surrounding elements and vegetation produce a precise result with lower average error in sunlight simulations (Sadeghi & Mistrick, 2022). The exterior surroundings can play a significant role as microclimatic modifiers. Consequently, they could reduce daylight availability of future crop-productive spaces on existing surfaces. Therefore, trees were incorporated as simplified forms considering differences in shape and height. Singapore’s case study was conducted first. The case study in India followed the methodology established in the first case study. Subsequently, a comparison between the simulated data in both locations was contrasted with the crop lighting thresholds specified in Section 2.1.3.

2.4.1. Singapore

According to the Köppen Climate Classification, Singapore has a Tropical Rainforest Climate (Af). This type of climate is usually found along the equator and has yearly stable conditions showing non-pronounced seasons. It is characterised by hot and wet weather, with similar monthly average temperatures throughout the year. The urban morphology of the Singapore University of Technology and Design campus consists of four buildings interconnected with elevated platforms and surrounding trees. The total ground area of the campus is 6.6 hectares. Buildings have a generalised height of 34 metres with lower sections of 6 to 12 metres. All buildings have flat rooftops, which can simplify the introduction of agriculture. However, most of the rooftop surface is occupied by machinery such as aircon facilities. A three-stage procedure was followed for the 3D model development: 3D scanning, scan processing and point cloud post-processing. First, 52 scans were performed with a 3D laser scanner

(Focus3D) and subsequently post-processed with Autodesk ReCap Pro to transform them into a 3D point cloud that was converted into surfaces using Rhino 3D modelling software.

2.4.2. Chennai. India

According to the Köppen Climate Classification, Chennai (India) has a Tropical Savanna Climate (Aw). In essence, this type of climate has a low seasonal variation in average temperatures and tends to see less rainfall than Singapore's climatic type, having more pronounced dry seasons. According to the sunlight analysis, this corresponds to higher yearly incident radiation levels. The urban morphology of the Hazur Garden area includes five buildings and many surrounding trees. The total ground coverage is 1.75 hectares, about one-quarter of the size of the Singapore campus. The buildings have a height of 6 to 12 metres and combine flat and slightly inclined rooftops. In this case, the 3D model was developed from the as-built construction plans data.

2.5. ANALYSIS OF SUNLIGHT DATA

This study proposes a three-dimensional methodology that considers all urban surfaces (rooftop, façade, ground) and interconnects the three factors under study: urban morphology, solar radiation, and crop lighting requirements. It links parametric and environmentally informed design toward higher use of solar radiation for urban agriculture planning and lighting optimisation in CEA. A sunlight simulation analysis was developed with the Ladybug analysis tool of Grasshopper graphical algorithm in Rhino software, using models of the case studies. A five-step procedure was set to perform the sunlight analysis: (1) import site-specific climatic data from the EPW file; (2) create a sky matrix; (3) set the analysis period (yearly period and 12-hour photoperiod from 7 am to 7 pm was established); (4) visualise the sky matrix under the selected period; and (5) realise the incident radiation study. The sunlight analysis considered four case scenarios separately: all surfaces, rooftop surfaces, facade surfaces, and ground surfaces. The results (see Figure 1) were analysed, and optimal locations for urban agriculture were selected according to solar radiation values, availability, and accessibility aspects. One of each type of surface was chosen to conclude common properties at each level (see Figure 2). Subsequently, an independent simulation was developed for these potential surfaces to deliver more refined results.

3. Results

The overall results of the sunlight simulations showed a prominent yearly quantity of average incident radiation on three-dimensional urban surfaces. The highest level of radiation is found on roofs, followed by non-shaded ground areas, while facades are the least solar-impacted (see Figure 1). The simulations developed on the selected surfaces (see Figure 2) showed finer results that can enable the location of specific crop species in each section of the grid (notice that a five-by-five-metre grid was superposed to divide the surface on a manageable crop scale). The comparison of results between the two case studies in Singapore and India (see Figure 1) highlights the impact of different boundary conditions (location, orientation, and surrounding elements) on sunlight simulations. The location determines the sun's path; consequently, the sunlight source's characteristics produce different results at varied locations. For this reason, in the case of Singapore, east facades are correlated with higher radiation values. In contrast, superior sunlight levels are found in Chennai's south-oriented facades (see Figure 2). In both locations, the impact of the surrounding elements (buildings, platforms, and trees) outweighs the orientation, blocking light and creating an overshadowing effect at the ground and façade surfaces. Concerning the overall values, simulations on potential areas (see Figure 3) show slightly higher values than those considering all urban surfaces, from which the highest total yearly incident radiation is found in Chennai.

The contrast between simulated data and the crop's lighting requirements (see Figure 1, Table 1) indicates three thresholds for crop environmental suitability that correspond to the roof, facade, and ground levels. In this case, Singapore facade locations could be suitable for crops with ID (1-2) and correspondent DLI between 0-2 mol·m-2·d-1, ground locations for crops with ID (3-6) and DLI 6-10 mol·m-2·d-1, and roof locations for crops with ID (7-16) and DLI 12-14 mol·m-2·d-1. In Chennai, the thresholds are coincident, including the possibility of Rubus idaeus (Raspberry) in roof areas. The previous data correlation indicates lighting thresholds for year-round harvesting on three-dimensional urban surfaces. The interconnection between the yearly sunlight data in selected surfaces (see Figure 2) and the crops' light requirements data (see Table 1) shows slightly different agricultural thresholds. In this case, the limits are coincident for both case studies. The selected facades could be suitable for crops with ID (1-3) and correspondent DLI between 0-6 mol·m-2·d-1, ground locations for crops with ID (4-17) and DLI 6-10 mol·m-2·d-1, and roof locations for crops with ID (18) and t DLI 18 mol·m-2·d-1. Lastly, species with ID (19-26) and DLI 20-32 mol·m-2·d-1 would require the application of artificial lighting for year-round crop production.

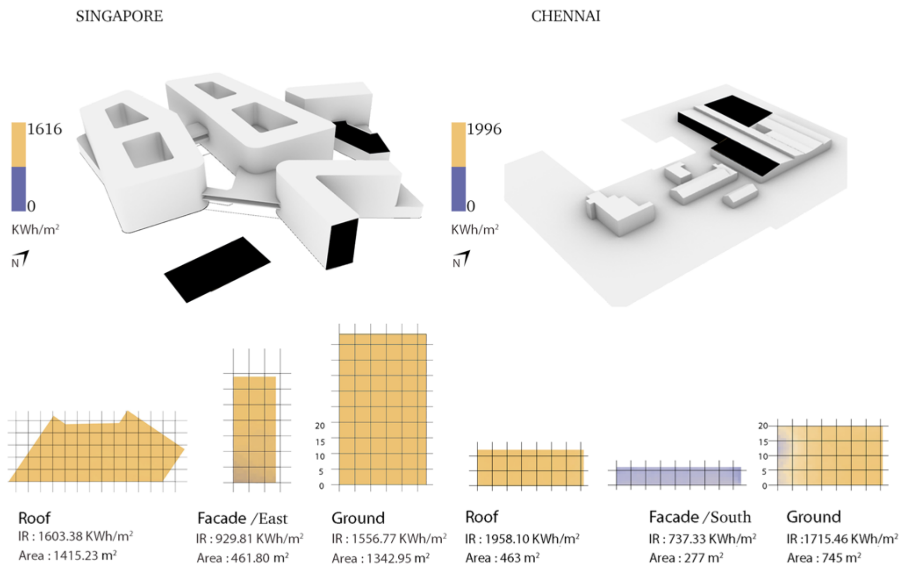

Figure 1:Results of the sunlight analysis.

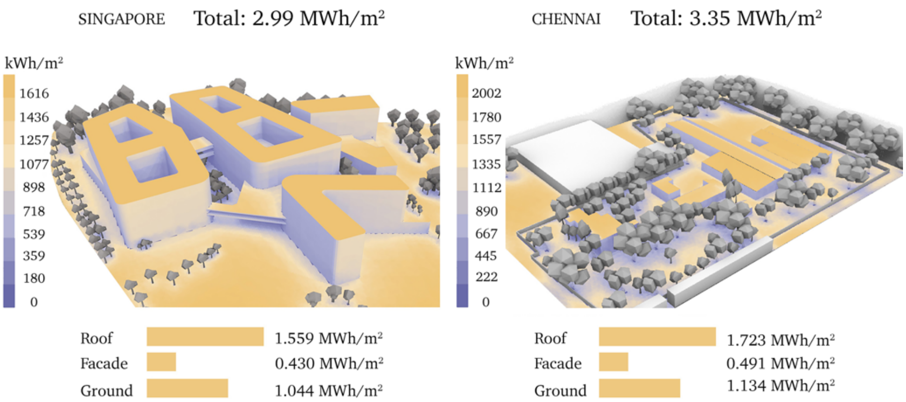

Figure 2: Upper part: Selected optimal surface locations for urban farming at the roof, façade, and ground levels. Bottom part: results of the sunlight analysis.

4. Discussion

The presented sunlight-based computational approach for crop-centric environmental suitability of agriculture on three-dimensional surfaces contributes to CEA urban planning and efficiency through passive natural lighting optimisation. The correlation of sunlight data and crops' DLI allows the establishment of sunlight thresholds for year-round harvesting on urban surfaces. These thresholds enable the integration of agriculture and buildings from an environmental and efficiency standpoint. It can be concluded that urban typologies of lower density and height offer the best performance on ground and rooftop areas. In comparison, higher density and height perform better on the facade. Additionally, the methodology generates a granular approximation to urban surfaces where even areas in shaded conditions can be exploited using species with low DLI requirements.

However, some limitations exist in this paper that can be developed in the future. First, instead of simulating annual data, future monthly or daily calculations may generate more accurate results and provide opportunities for seasonal climatic adaptation of CEA. For instance, the results showed that crops with DLI 20 mol.m-2.d-1 and above (see Table 1) require artificial lighting for year-round harvesting. Conversely, with monthly calculations for these types of crops, seasonal harvesting can be organized to achieve higher artificial lighting efficiency. Second, cover materials decrease the amount of light inside controlled environment spaces. Consequently, the lighting thresholds should change accordingly depending on the level of transmittance of the enclosure material. Third, simulations can underestimate sunlight values due to several factors, such as using weather forecast data instead of real-time weather conditions (Palliwal et al., 2021). For this reason, some crops with low DLI requirements can develop growth difficulties under higher lighting environments. Nevertheless, most species have improved growth behaviour under higher lighting conditions (Currey & Yost, 2020).

This paper demonstrates the capacity of three-dimensional food production on urban surfaces. The methodology's broader implications foster food security in cities by classifying urban surfaces according to crop-specific production lighting requirements. As a result, this method can support designers (architects, urban planners, and engineers) and local governments in strategizing urban farming developments and provide decision-making support for crop-harvesting initiatives in cities. Furthermore, urban agriculture has several advantages, including reducing energy consumption in CEA systems, crop yield enhancements with predictable outputs, better food quality, promotion of healthy diets, as well as improved food production chains. These advantages benefit the sustainability of urban environments, affecting their environmental, social, and economic conditions. Ultimately, sustainable local food systems significantly help mitigate climate change by reducing environmental degradation and deforestation, a consequence of extensive agricultural processes.

Acknowledgements

The authors would like to thank Singapore University of Technology and Design students: Sunilkarthik Ezhilarasu from the Master of Innovation by Design (Engineering Product Development) and Madhumita Gokuldas Kumar from the Master of Architecture (Architecture and Sustainable Design). For their collaboration on the sunlight simulations (see Figures 1 and 2).

References

Currey, C. J., Walters, K. J. & Flax, N. J. (2019). Nutrient solution strength does not interact with the daily light integral to affect hydroponic cilantro, dill, and parsley growth and tissue mineral nutrient concentrations. Agronomy, 9(7), 1–14. https://doi.org/10.3390/agronomy9070389

Currey, C. J. & Yost, J. (2020). Managing the Daily Light Integral for Specialty Leafy Greens. Controlled Environment Agriculture, October, 1–2.

Despommier, D. (2010). The Vertical Farm: Feeding the World in the 21st Century. Picador Press.

Dou, H., Niu, G., Gu, M. & Masabni, J. G. (2018). Responses of sweet basil to different daily light integrals in photosynthesis, morphology, yield, and nutritional quality. HortScience, 53(4), 496–503. https://doi.org/10.21273/HORTSCI12785-17

Engler, N. & Krarti, M. (2021). Review of energy efficiency in controlled environment agriculture. Renewable and Sustainable Energy Reviews, 141(January), 1–12. https://doi.org/10.1016/j.rser.2021.110786

Fondriest Environmental, Inc. (2014). Fundamentals of Environmental Measurements: Solar Radiation and Photosynthetically Active Radiation. Fondriest, Environmental Learning Centre. Retrieved September 27, 2022, from https://www.fondriest.com/environmental-measurements/parameters/weather/solar-radiation/

Gellenbeck, S., Pryor, B., Giacomelli, G. & Rd, R. (2019). Mushrooms on Mars: A Subsystem for Human Life Support. 49th International Conference on Environmental Systems, ICES 2019, 1–11. American Institute of Aeronautics and Astronautics. https://ttu-ir.tdl.org/handle/2346/84470

Irulegi, O., Torres, L., Serra, A., Mendizabal, I. & Hernández, R. (2014). The Ekihouse: An energy self-sufficient house based on passive design strategies. Energy and Buildings, 83, 57–69. https://doi.org/10.1016/j.enbuild.2014.03.077

LEDTonic. (n.d.). DLI (Daily Light Integral) Chart - Understand your plants' PPFD & photoperiod requirements. LEDTonic. Retrieved 2 November 2022, from https://www.ledtonic.com/blogs/guides/dli-daily-light-integral-chart-understand-your-plants-ppfd-photoperiod-requirements

Mavi, H. S. & Tupper, G. J. (2004). Agrometeorology: principles and applications of climate studies in agriculture. Food Products Press. https://doi.org/10.5860/choice.42-3406

Nadal, A., Alamus, R., Pipia, L. & Ruiz, A. (2017). Urban planning and agriculture. Methodology for assessing rooftop greenhouse potential of non-residential areas using airborne sensors. Science of the Total Environment, 601–602, 493–507.

Palliwal, A., Song, S., Tan, H. T. W. & Biljecki, F. (2021). 3D city models for urban farming site identification in buildings. Computers, Environment and Urban Systems, 86(2021), 1–16. https://doi.org/10.1016/j.compenvurbsys.2020.101584

Sadeghi, R. & Mistrick, R. (2022). The Impact of Exterior Surround Detail on Daylighting Simulation Results. Leukos- Journal of Illuminating Engineering Society of North America, 18(3), 341–356. https://doi.org/10.1080/15502724.2021.1947313

Saha, M. & Eckelman, M. J. (2017). Growing fresh fruits and vegetables in an urban landscape: A geospatial assessment of ground level and rooftop urban agriculture potential in Boston, USA. Landscape and Urban Planning, 165(August 2016), 130–141. https://doi.org/10.1016/j.landurbplan.2017.04.015

Specht, K., Siebert, R., Hartmann, I., Freisinger, U. B., Sawicka, M., Werner, A., Thomaier, S., Henckel, D., Walk, H. & Dierich, A. (2014). Urban agriculture of the future: An overview of sustainability aspects of food production in and on buildings. Agriculture and Human Values, 31(1), 33–51. https://doi.org/10.1007/s10460-013-9448-4

Torres, A. P. & Lopez, R. G. (2012). Measuring Daily Light Integral in a Greenhouse. Purdue Extension. Horticulture, HO-238-W, 1–7. www.hort.purdue.edu

Trnka, M., Eitzinger, J., Kapler, P., Dubrovský, M., Semerádová, D., Žalud, Z. & Formayer, H. (2007). Effect of estimated daily global solar radiation data on the results of crop growth models. Sensors, 7(10), 2330–2362. https://doi.org/10.3390/s7102330

Weiss, A. & Norman, J. M. (1985). Partitioning Solar Radiation into Direct and Diffuse, Visible and Near-Infrared Components. Agricultural and Forest Meteorology, 34, 205–213.

Zhu, R., Wong, M. S., Kwan, M. P., Chen, M., Santi, P. & Ratti, C. (2022). An economically feasible optimization of photovoltaic provision using real electricity demand: A case study in New York city. Sustainable Cities and Society, 78(January), 1–15. https://doi.org/10.1016/j.scs.2021.103614

Zhu, R., Wong, M. S., You, L., Santi, P., Nichol, J., Ho, H. C., Lu, L. & Ratti, C. (2020). The effect of urban morphology on the solar capacity of three-dimensional cities. Renewable Energy, 153, 1111–1126. https://doi.org/10.1016/j.renene.2020.02.050